

Effect of Different Types of Terpenes on Disulfiram Loaded Transdermal Invasomes Preparation and *in-vitro* Characterization

Worood Hameed AL-Zheery¹  and Hanan Jalal Kassab^{*2} 

¹ Department of Pharmaceutics, College of Pharmacy, Al-Esraa University, Baghdad, Iraq.

² Department of Pharmaceutics, College of Pharmacy, University of Baghdad, Baghdad, Iraq.

***Corresponding author**

Received 19/12/2023, Accepted 25/4/2024, Published 20/9/2025



This work is licensed under a Creative Commons Attribution 4.0 International License.

Abstract

Invasomes are innovative vesicular structures that exhibit enhanced transdermal permeation in comparison with traditional liposomes. The structure of these vesicles consists of phospholipids, ethanol, and terpene. These components provide soft invasome vesicles that can penetrate the skin easily. Disulfiram (DSF) is a thiocarbamate derivative that has been employed for the treatment of alcoholism and can also be utilized for the treatment of tumors. The objective of this study is to develop a Disulfiram invasome as a vesicular carrier and evaluate the effect of various formulation variables, such as the type and quantity of terpenes (limonene, citral, and carvacrol), on the particle size, entrapment efficiency (EE), and polydispersity index (PDI) of the invasomes which are prepared. The optimized invasomal dispersion with EE > 70 % was chosen for the *in vitro* release study. DSF-loaded invasomes were successfully prepared by the thin film hydration technique. Nine invasome formulations were developed to prepare DSF invasomal dispersion. The selected invasomal dispersion (DSF-IV8) that has a higher % of DSF release was further analyzed for its zeta potential, compatibility study by Fourier transforms infrared spectroscopy (FTIR), and morphology by Transmission electron microscopy (TEM). The DSF-IV8 invasome, which is composed of DSF, soya phosphatidylcholine (2%), carvacrol (1% w/v), and ethanol (40% v/v), demonstrated optimal characteristics, including spherical vesicles having a particle size of 119.2 ± 2.2 nm, a PDI of 0.18 ± 0.05 , and an EE of $95.3 \pm 0.8\%$ and 96.32% of DSF release from invasomal dispersion after 24 hours, the zeta potential value was measured to be -33.6 ± 1.6 mV, (FTIR) analysis showed the compatibility between the drug and other excipients in the formula. TEM image as intact, spherical vesicles with a distinct shape and core, free of any clumping, and exhibiting well-defined internal characteristics. Eventually, the thin film hydration approach was shown to be effective in formulating invasomal dispersion.

Keywords: Transdermal delivery, Invasome, Disulfiram, Terpenes, carvacrol

Introduction

Transdermal delivery involves the application of a drug formulation onto the skin to allow for its absorption into the bloodstream. The process is completely painless and involves the penetration of drugs from the outermost layer of the skin (stratum corneum) into the underlying layers, the epidermis and dermis, where they can be absorbed into the bloodstream ⁽¹⁾. The transdermal drug delivery system provides numerous benefits, such as the ability to self-administer the drug and achieve a consistent and sustained release. This results in steady levels of the drug in the bloodstream throughout the entire administration period. Additionally, it avoids enzymatic degradation in the gastrointestinal tract, thereby preventing any side effects associated with the gastrointestinal tract. Moreover, it serves as an alternative route for patients unable to take oral medication. Lastly, the administration of the medication concludes when the formula is removed

from the skin surface ⁽²⁾. One of the current approaches is to overcome the barrier function of SC by using various delivery systems for drugs, including nanodrug delivery systems such as nanoemulsions, liposomes, solid lipid nanoparticles, and nanostructured lipid carriers ⁽³⁾. Novel nano drug delivery systems have been adopted recently as promising delivery systems to enhance drug penetration through the skin, such as niosome (prepared mostly by non-ionic surfactant and cholesterol) and ethosome (containing high amounts of ethanol in their structure) ⁽⁴⁾. Invasomes are innovative vesicular systems that play an important role in improving transdermal penetration of active drug molecules as compared to other conventional vesicles. These vesicles are composed of phospholipids, ethanol, and terpene or a mixture of terpenes in their structures. These components worked as suitable transdermal penetrators with good penetration properties. Invasomes are bilayer

vesicles, comprised of soya phosphatidylcholine (SPC), lysophosphatidylcholine (flexibility substances), terpenes, and ethanol (permeation enhancer). The invasome's composition is represented in deeper skin medication levels, achieving synergistic alterations and allowing invasomes to possess soft and flexible properties in all components (i.e., unsaturated phospholipids, terpenes, and ethanol) than in the case of traditional liposomes or a drug solution^(5,6).

Terpenes, a main component of invasomes, can promote skin penetration. They are used in pharmaceutical formulations to give a transdermal release, the mechanism of terpenes as penetration enhancers, breaking the lipid sealing of the SC (stratum corneum) and boosting transepidermal osmotic concentration through the hair follicles⁽⁷⁾. Disulfiram (DSF) is a thiocarbamate derivative that has been employed for the treatment of alcoholism and can also be utilized for the treatment of tumors. DSF can serve as a modulator to effectively counteract multidrug resistance⁽⁸⁾. Although DSF offers specific benefits in the treatment of tumors, it is also accompanied by notable limitations such as poor solubility in biological fluids, a short half-life in the bloodstream, and the absence of any cytotoxic effects on cancer cells when metabolized by hepatic enzymes^(9,10). Oral DSF is associated with several gastrointestinal side effects, such as nausea and vomiting. In the case of the poor stability of DSF in the gastric environment and its side effects, the development of more effective drug delivery systems is necessary. DSF is a lipophilic drug with a molecular weight of approximately 296.54, an oil-water partition coefficient of 3.9, and a melting point range from 70 -74 °C, so it meets the conditions of established transdermal preparations⁽¹¹⁾.

Previous studies showed that various nanocarriers for DSF have been explored, including DSF/nanomicelles^(12,13), DSF/nanosuspensions⁽¹⁴⁾, DSF / Lactoferrin nanoparticles⁽¹⁵⁾, DSF/PEGylated liposomes⁽¹⁶⁾, DSF/micelle microneedles⁽¹⁷⁾, and DSF/niosome⁽¹⁸⁾.

The objective of the present study is to produce invasomes vesicles containing DSF, which

is a crucial first stage in the development of transdermal dosage forms. The invasomal dispersion was primarily evaluated for their vesicle size, polydispersity index, entrapment efficiency of DSF in the vesicles, and in vitro drug release. The dispersions that exhibited greater entrapment of DSF and possessed vesicle sizes within the nano-size range, as well as higher percentages of DSF release, were selected for further investigation.

Materials and Methods

Materials

Disulfiram was obtained from Hyper Chem for Chemicals, China. Absolute ethanol, methanol, KH₂PO₄, and NaOH were purchased from Chem-Lab, Belgium. Chloroform, limonene, and carvacrol were purchased from Bide Pharmaceutical Ltd. (China), and the citral was obtained from Jiangxi Yisenyuan Plant Spice Co., Ltd. (China). Soybean phosphatidylcholine with a purity of >90% and mannitol (China) was used. All other chemicals and solvents used in this study were of analytical grade.

Preparation of DSF-Loaded Invasomes

Disulfiram nanoinvasome formulations are produced using the traditional thin film hydration method⁽¹⁹⁾. Accurately weighted amounts of (2% w/v) Soybean phosphatidylcholine (SPC90), DSF (5 mg/mL), and different types and % of terpenes (limonene, citral, or carvacrol), were dissolved in a mixture of 8:4 ml methanol: chloroform, which was thereafter placed into a dry, clean 100 mL round-bottom flask and completely mixed. The organic solvent was evaporated by a rotatory evaporator (Buchi rotary evaporator, Germany), rotating at 90 rpm at 40 °C for 30 min under low pressure to obtain a clear film on the walls of the flask. The deposited lipid film was then hydrated by phosphate buffer (pH 7.4)- ethanolic solution (6:4) ml mixture by rotation at 120 rpm for 1 h at 50 °C⁽²⁰⁾. For particle size reduction and homogenization, the suspension was probe sonicated at 4 °C at 20% output frequency for 5 min. Table 1 shows the nine distinct formulations prepared and stored at 4 °C for later use⁽²¹⁾.

Table 1. The Composition of different DSF-loaded invasomes formulations

Code	Drug mg/ml	SPC 90(w/v) %	Terpene type	Terpene concentration (%w/v)	Ethanol Ml	PB (7.4) ml	Hydration Volume (ml)
DSF-IV1	5	2	Limonene	0.5	4	6	10
DSF-IV2	5	2	Limonene	1	4	6	10
DSF-IV3	5	2	Limonene	1.5	4	6	10
DSF-IV4	5	2	Citral	0.5	4	6	10
DSF-IV5	5	2	Citral	1	4	6	10
DSF-IV6	5	2	Citral	1.5	4	6	10
DSF-IV7	5	2	Carvacrol	0.5	4	6	10
DSF-IV8	5	2	Carvacrol	1	4	6	10
DSF-IV9	5	2	Carvacrol	1.5	4	6	10

Determination of the particle size and polydispersity index

The size and distribution of prepared invasomes were measured using dynamic light scattering (DLS) by Malvern Zetasizer (Malvern Zetasizer, Ultra rate Company, UK) at a temperature of $25 \pm 2^\circ\text{C}$. After a suitable dilution with deionized water, the invasomal dispersion was measured to ensure that the light scattering intensity was within the instrument's sensitivity range. The measurements involve particle size (PS) and polydispersity index (PDI); all of the measurements were performed in triplicate, and the mean values obtained were reported^(22,23).

Determination of Entrapment Efficiency (EE%)

The EE% of DSF in the invasomal dispersion was determined using the direct methods. A volume of one ml of the invasomal dispersion was placed in a cooling centrifuge and subjected to centrifugation for one hour at a speed of 15,000 rpm at a temperature of 4°C . The DSF-loaded invasomes were lysed and solubilized by sonication with ethanol. The resulting solution was subsequently diluted and analyzed using spectroscopy at λ_{max} 217 nm. Measurements were taken in triplicate, and a percentage of the encapsulation efficiency (EE%) was calculated according to^(24,25).

EE%

$$= \frac{\text{Entrapped amount of DSF (mg)}}{\text{Total amount of DSF (mg)}} \times 100$$

In vitro drug release

Optimized invasomes dispersions with higher entrapment efficiency ($\geq 70\%$) were evaluated for the in vitro release study of DSF. The release was done to three invasomal dispersions that contain higher EE% of DSF (DSF-IV7, DSF-IV8, and DSF-IV9), which contain carvacrol (0.5, 1 and 1.5%) respectively, and pure DSF using a dialysis membrane with a molecular weight cutoff range of 12,000-14,000 Da, obtained from Sigma, Aldrich in St. Louis, MO, USA⁽¹⁸⁾. The membrane was soaked in the release media overnight before the study, and the release was examined using the type II dissolution devices. The dialysis bags were immersed in 250 mL of buffer solution with a pH of 7.4 at 37°C . At fixed time intervals of 0.25, 0.5, 1, 2, 4, 8, 12, 16, 20, and 24 hours, 3 mL samples of the medium were obtained and substituted with an equivalent volume of fresh medium to maintain a constant sink condition. The amount of drugs released into the buffer was calculated using a UV-vis spectrophotometer (UV-1900i, Shimadzu, Japan) at a wavelength of 217 nm.^(26,27)

Optimum formula selection

The optimum formula was chosen based on the results of the following tests: lower particle size analysis, good polydispersity index (PDI), higher encapsulation efficiency (EE%), and the highest % DSF released after 24 h. The optimized formulation was found to be DSF-IV8 with carvacrol as the

terpene in a concentration of 1%. Therefore, DSF-IV8 was selected and was further evaluated for zeta potential Z.P., Differential scanning calorimetry (DSC) analysis, compatibility study by Fourier-transform infrared spectroscopy (FTIR) analysis, and morphology by the transmission electron microscope (TEM).

Measurement of zeta potential for the selected formulas

Zeta potential (ZP) was used to determine whether the charged particles were repelling or attracting one another, and the surface charge of the produced vesicles was measured in terms of zeta potential by the measurement of the electrophoretic mobility of the particles. The measurement of DSF-IV8 was performed via the Zetasizer ZS90 apparatus supplied by Malvern, UK. According to requirements, the samples were diluted using deionized water as the solvent, and scanning was conducted at a temperature of 25°C with an angle of scattering at 90° ⁽²⁸⁾.

Lyophilization of optimized formulation

Lyophilization of optimized formulation (DSF-IV8) was performed using 5% (w/v) mannitol as a cryoprotectant and then lyophilized for 48 h. The pressure was set at 0.4 bar in the Labconco Free Zone Benchtop freeze dryer (USA)⁽²⁹⁾.

Differential scanning calorimetry (DSC) analysis

The DSF formulation performed thermal examination using a Differential Scanning Calorimeter (DSC-60 plus, Shimadzu, Japan) to determine the presence of any interactions between the DSF and the excipients. A study was carried out to assess the thermal properties of four substances: pure DSF, SPC90, a physical blend of DSF, and the lyophilized optimized formulation (DSF-IV8). Meticulously measured and preserved each sample in aluminium pans while being shielded by a layer of nitrogen gas. Afterwards, we exposed the samples to a controlled heating rate of 10°C per minute and a cooling rate of 40°C per minute in the temperature range of 0 - 300°C . The reference object was a blank aluminium pan^(30,31).

Fourier-transform infrared spectroscopy (FTIR) analysis

The DSF compatibility with the invasomal components was assessed by Fourier-transform infrared spectroscopy (FTIR). Analyzed using a PerkinElmer FT-NIR spectrometer from the USA, the spectra of DSF, SPC90, and a physical mixture of DSF: SPC90 with a weight ratio of 1:1 were obtained and examined with FTIR. After compression, each specimen was inserted into a disc and underwent scanning from 4000 cm^{-1} to 500 cm^{-1} . The selected liquid formula was placed directly, and the FTIR spectrum of it was obtained using the same device⁽³²⁾.

Examination of the morphology using the transmission electron microscope (TEM)

The morphology of the optimal formulations was analyzed using a Philips EM208 transmission electron microscope (TEM). The carrier dispersion was deposited as a thin film onto a copper grid that had been coated with carbon. The film was then stained using a 1% phosphotungstic acid solution and subsequently observed and captured ⁽³³⁾.

Statistical analysis

The study's results were subjected to rigorous statistical and scientific analysis using GraphPad Prism version 10.1.0(316). Several statistical approaches, such as paired sample t-tests and ANOVA (analysis of variance), were used for analyzing and interpreting the results. To qualify for the results to be considered statistically significant, the p-values must be less than 5% ($p < 0.05$).

Results and Discussion

Determination of particle size

According to a recent study, lipid-based vesicles with a diameter of 300 nm or smaller can transport their contents to the deeper layers of the skin, particularly when flexible ⁽³⁴⁾. Table 2 displays the estimated PS (particle size) and PDI (polydispersity index) values for the nine nanoinvasomes formulas that were developed throughout an optimization process. All produced vesicles possess a diameter that constantly falls within the nanometres range, which is essential to effectively penetrate the skin and enter the bloodstream. The nanovesicles ranged in size from 105.8 ± 7.6 nm to 283.9 ± 12.7 nm, with the smallest and largest sizes observed ⁽³⁵⁾; among all formulations, DSF-IV8 displayed particle size (119.2 ± 2.2 nm). The particle size and amount of drug present in nanovesicles are influenced by several factors, including the chemical structure, quantity and nature of the drug, lipid composition, and experimental procedures ⁽³⁶⁾. The effect of terpene on invasome size was significant ($p < 0.05$), as shown in Fig.1. Increasing the concentration of limonene and citral in the formulation resulted in an enlargement of the particle size. Elevated levels of terpenes would lead to an excessive fluidity of the cell membrane, promoting the merging of vesicles and subsequently causing an enlargement of the vesicles ⁽³⁷⁾.

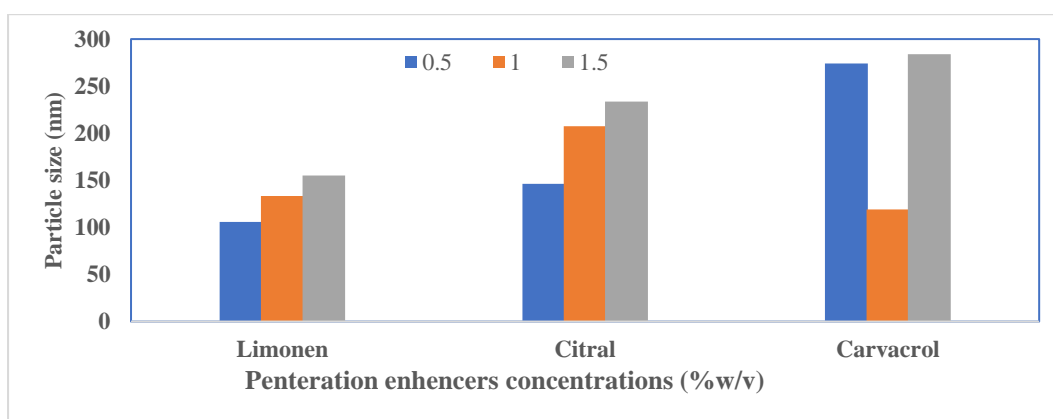
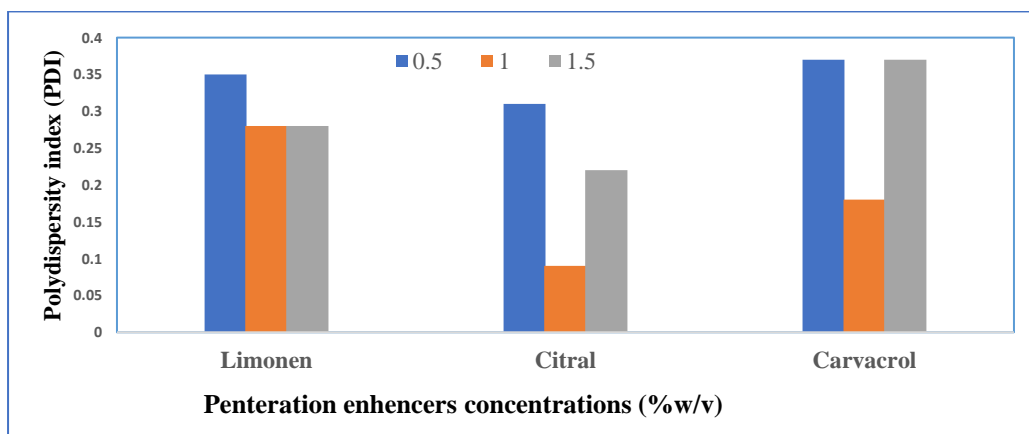
Since the size of the vesicles is closely proportional to the molecular size of terpenes, this observation may be explained by the structural dependence of invasome particle size. The molecular sizes of limonene and citral are 136.24 g/mol and 152.24 g/mol, respectively. As a result, there are noticeable variations in particle size among invasomal vesicles that contain the same concentration of any of these terpenes ⁽²⁰⁾. Also, the concentration of carvacrol has a direct relation with

particle size, with significant ($p < 0.05$), carvacrol molecular sizes (150.217 g/ mole) containing soft nanovesicles displayed the smallest vesicle sizes compared to limonene and citral containing the same concentration ⁽³⁸⁾. For both terpenes' concentration and terpenes type, the factors had a significant effect ($p < 0.05$) ⁽³⁹⁾. The reduction in size resulting from the carvacrol concentration is linked with changes in molecular interactions inside the membrane induced by phenolic compounds. These facilitated changes in the structure of the membrane, resulting in modifications in the size of the vesicles and the polydispersity index (PDI). The size fluctuations were determined by the molecular configuration (size and shape), polarity, and chemical attraction of the phenolic substances being loaded. Phenolic compounds that include phenolic hydroxyl groups can interact synergistically with the polar heads of lipids, resulting in changes in the structure of the membranes ⁽⁴⁰⁾.

At higher concentrations of terpene, an increase in particle size was found, indicating a correlation between the concentration of penetration enhancer and particle size ⁽⁴¹⁾. This phenomenon may be attributed to the inclusion of terpenes in the lipid bilayer membrane of the invasomes, which disrupts its cohesive arrangement. Greater concentrations of terpenes necessitate a bigger surface area of the membrane to accommodate them, resulting in the production of larger invasomes. This suggests that the size of the vesicles increases as the amount of terpenes within them rises ⁽⁴²⁾. The measured polydispersity index (PDI) values for the analyzed DSF-invasomal formulations varied from 0.09 ± 0.06 to 0.37 ± 0.09 , as shown in Figure 2. The results confirmed that all the DSF-invasomal vesicles produced exhibit an appropriate homogeneity in size distribution with a significant effect ($p < 0.05$) for both terpene type and concentration ^(43,44).

Table 2. Particle size, polydispersity index, and Entrapment efficiency measurements of DSF-loaded invasomes (mean \pm SD, n=3)

Code	Particle size (nm)	Polydispersity Index (PDI)	Entrapment efficiency (%EE)
DSF-IV1	105.8 \pm 7.6	0.35 \pm 0.03	38.3 \pm 0.8
DSF-IV2	133.4 \pm 9.15	0.28 \pm 0.05	35 \pm 0.7
DSF-IV3	155 \pm 8.31	0.28 \pm 0.04	31.6 \pm 0.43
DSF-IV4	146.1 \pm 4.1	0.31 \pm 0.1	52 \pm 0.7
DSF-IV5	207.5 \pm 0.4	0.09 \pm 0.06	46 \pm 0.72
DSF-IV6	233.7 \pm 4.6	0.22 \pm 0.09	42 \pm 1.08
DSF-IV7	274 \pm 33.7	0.37 \pm 0.09	86.3 \pm 0.83
DSF-IV8	119.2 \pm 2.2	0.18 \pm 0.05	95.3 \pm 0.8
DSF-IV9	283.9 \pm 12.7	0.37 \pm 0.07	77 \pm 0.71

**Figure 1. The effect of different types of penetration enhancers (Limonene, Citral, Carvacrol) on the particle size of invasomes.****Figure 2. The effect of different types of penetration enhancers (Limonene, Citral, Carvacrol) on the polydispersity index.****Entrapment efficiency (EE%)**

The drug's capacity to incorporate lipid content and form stable vesicles, as well as the dependency on penetration enhancers, primarily determines the percentage of drug entrapped in the vesicles. This dependence is largely influenced by the physical and chemical characteristics of the drug. The entrapment efficiency of DSF in various invasomal formulations varied between 31.6 \pm 0.43% and 38.3 \pm 0.8% for limonene, 42 \pm 1.08% and 52 \pm 0.7% for citral, and 77 \pm 0.71% and 86.3 \pm 0.83%

for carvacrol, as shown in Figure 3. The formulation DSF-IV8, which consisted of 2% PC90, 40% ethanol, and 1% carvacrol, had the highest efficiency in terms of %EE, with a maximum value of 95.3 \pm 0.8%. The significant trapping of DSF within the invasomal formula (DSF-IV8) can be attributed to its multi-lamellarity and the effect of ethyl alcohol with SPC90 concentration⁽⁴³⁾. The effect of terpene concentration on entrapment efficiency was statistically significant ($p < 0.05$). Concerning the influence of terpene concentration

on the entrapment efficiency percentage, it was shown that higher concentrations of terpenes had an adverse impact on the entrapment efficiency of DSF. The decrease in the entrapment of DSF may be attributed to the competition between lipophilic drugs and terpenes for incorporation into the lipid bilayer of the vesicle⁽⁴⁵⁾. The variation in carvacrol terpene types is attributed to their distinct characteristics, including structural differences, molecular weight variations, and differences in lipophilicity. These distinctions facilitate the investigation of the impact of terpene characteristics⁽⁴¹⁾.

The EE% of all invasomes is correlated with the logarithm of the partition coefficient (log P) value, which includes carvacrol (log P = 3.52), citral (log P = 3.17), and limonene (log P = 4.83). Carvacrol exhibited a higher percentage of encapsulation efficiency (%EE) compared to DSF due to its log P value being close to that of DSF. The

%EE values for carvacrol were $86.3 \pm 0.83\%$ (DSF-IV7), $95.3 \pm 0.8\%$ (DSF-IV8), and $77 \pm 0.71\%$ (DSF-IV9) respectively⁽²⁹⁾. Citral and limonene followed carvacrol in terms of %EE as shown in Table 2. The observed result could be attributed to the solubility of DSF within the lipid bilayers. Given that the logarithm of the partition coefficient (log P) of DSF is 3.88, it is likely to be soluble in a composition with a similar value.^(38,39) Regarding the concentration of terpenes, there were significant reductions in the DSF EE% as the terpene concentration increased from 0.5% w/v to 1.5% w/v for limonene and citral. As the terpene concentration increases, the invasomes become more fluid, resulting in a decrease in the drug's EE%. In addition, enhancing the quantity of terpenes could lead to the creation of holes that might destabilize the lipid bilayers of invasome thus lowering the values of EE%⁽²⁵⁾.

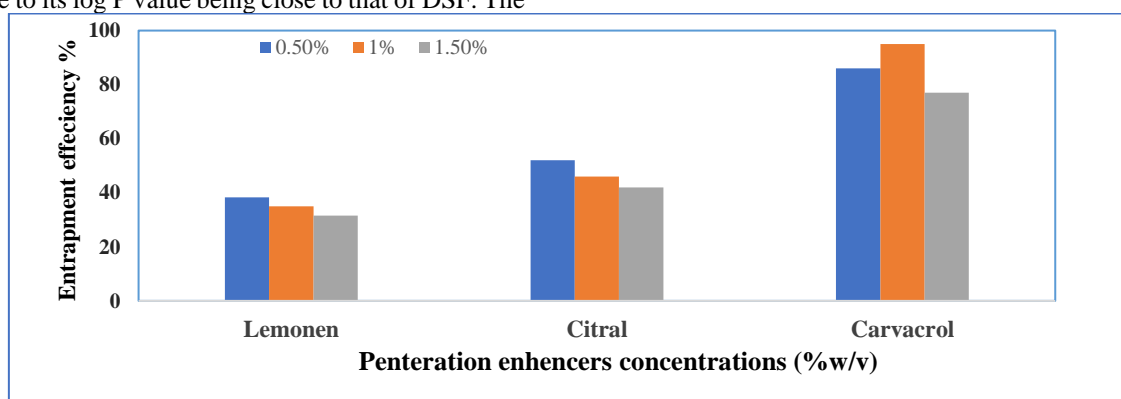


Figure 3. Effect of Penetration Enhancer concentration on entrapment efficiency of invasomes.

In vitro release studies

The release profiles of DSF from different DSF-loaded invasomes are presented in Fig. 4. Results of the ANOVA analysis show that carvacrol concentration had a significant impact (p -value < 0.05) on the % DSF release after 24 hrs. The rapid initial release within the first two hours, (15.1%, 24.3%, and 12.3%) may be attributed to the DSF being absorbed onto the surface of nanovesicles, facilitated by their high surface-to-volume ratio, following the initial rapid release phase, a regular and gradual release of the drug was observed over the next 24 hours (77.2%, 96.3%, and 73.1%) for formula (DSF-IV7, DSF-IV8, and DSF-IV9 respectively). This indicates a continuing and prolonged release of the drug, which can be attributable to the mechanisms of drug diffusion and matrix erosion⁽¹⁸⁾. Data showed that all invasomal

dispersions exhibited an extended-release behaviour over 24 hours, and all invasomal dispersions had a higher % of DSF release in comparison with the pure drug due to the solubilizing effect of invasomes, leading to enhanced drug release and the aqueous solubility.

The order of drug release from a lower % of DSF release to higher (DSF-IV8, DSF-IV7, and DSF-IV9), the invasomal dispersion DSF-IV8 having a higher % of DSF release likely explanation might be due to the smaller particle size of the invasomes⁽⁴⁶⁾. Increased concentration of carvacrol up to 1% leads to increased drug release for invasome dispersion DSF-IV7 and DSF-IV9, but very high concentrations of carvacrol, 1.5% may also destabilize the invasome structure and lead to premature drug release^(47,48,49).

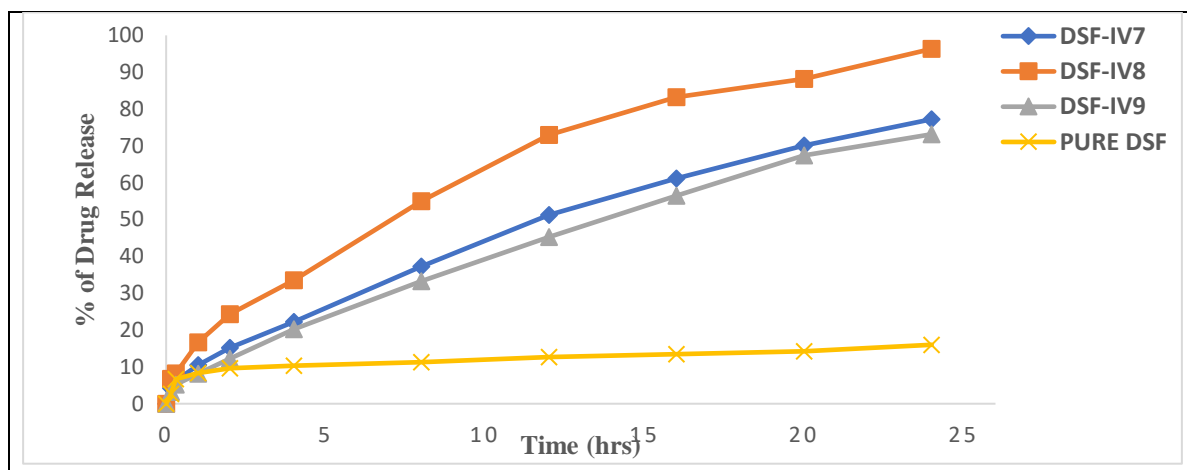


Figure 4. In Vitro, the release profile of DSF from DSF-loaded invasomes was prepared using carvacrol at different % and pure disulfiram.

Optimization of DSF invasomal dispersion

The optimized DSF-invasomes formulation was obtained from DSF-IV8 with the 119.2 ± 2.2 nm vesicle size, 0.18 ± 0.05 PDI, and $95.3 \% \pm 0.8\%$ EE% and 96.32% of DSF was released with sustained over 24 hours, also includes a high concentration with penetration enhancers (1% carvacrol), which is required for optimum transdermal delivery.

Zeta potential

Invasomes are vesicular systems characterized by their negatively charged surfaces,

which are attributed to the presence of ethanol and phosphatidylcholine. The zeta potential of the optimum formulation, as shown in Figure 5, was measured and found to be -33.6 ± 1.6 mV. This high negative charge is attributed to the presence of ethanol, which provides a net negative surface charge and prevents vesicle aggregation due to electrostatic repulsion. These results ensure the stability of invasomal dispersion and the avoidance of aggregation of the nanovesicles⁽⁵⁰⁾.

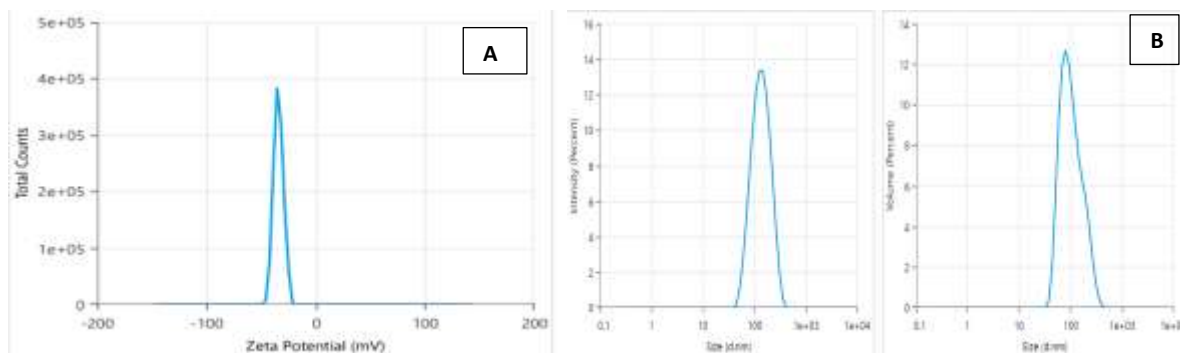


Figure 5. A) Zeta potential, B) Vesicle size distribution, for DSF-IV8

Differential scanning calorimetry (DSC)

The thermograms showing the pure drug, the physical mixing of the drug and other components, and the lyophilized DSF-IV8 may be observed in Figure 6. The thermogram of the pure DSF sample exhibited a distinct and intense endothermic peak at a temperature of 74.21°C . (Figure 6A) The observed peak may correspond to the melting point of DSF,

demonstrating its crystalline state. On the other hand, the peak measured at around 195°C corresponds to its thermal degradation. However, the absence of a distinct peak (at 74.21°C) for the "guest" molecule (DSF) in thermograms of the lyophilized DSF-IV8 could be due to indicating that the crystalline form has been converted to the amorphous form^(51,52).

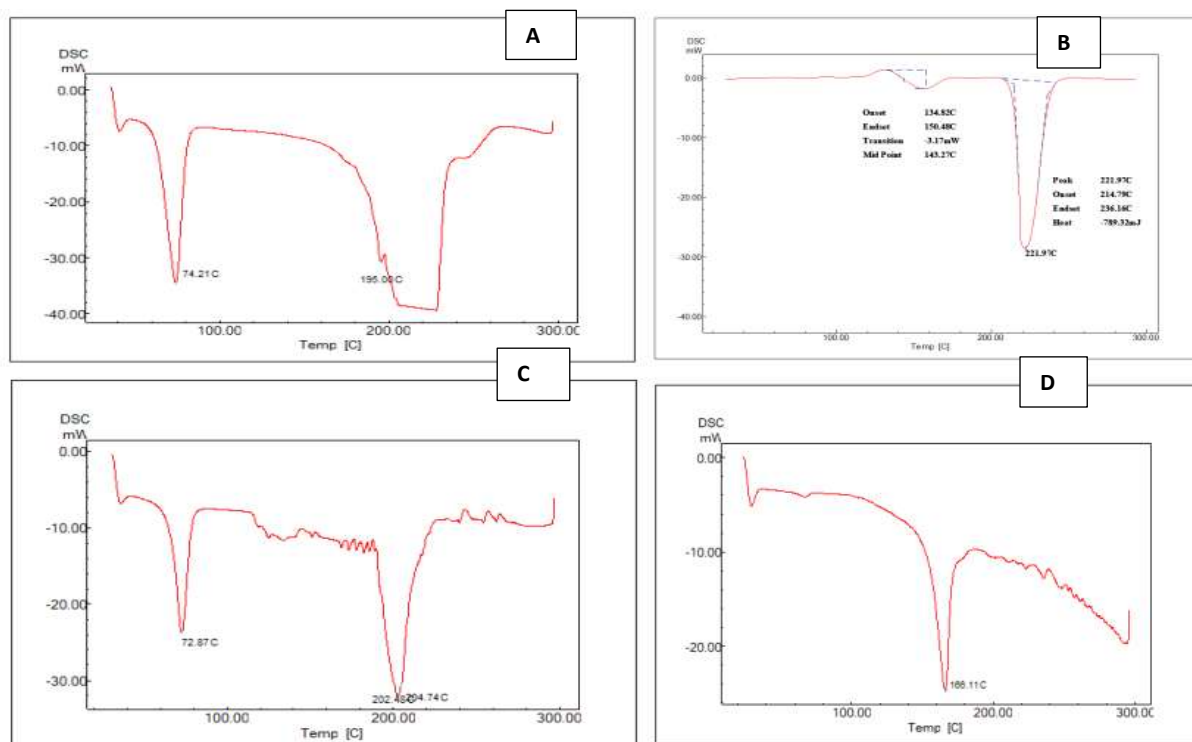
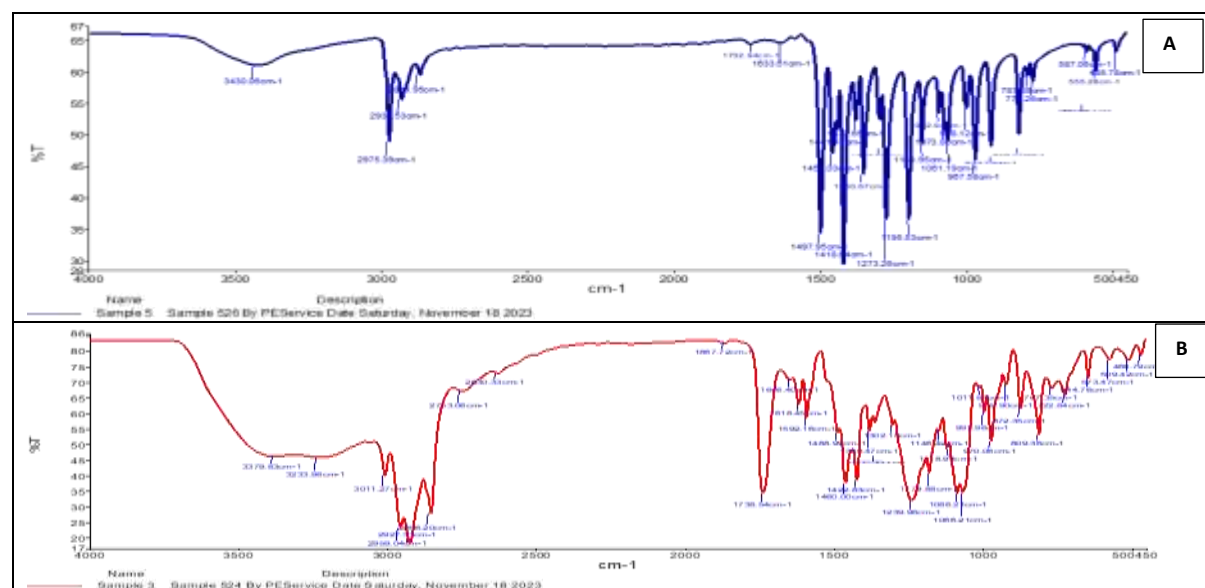


Figure 6. DSC thermogram (A) pure DSF (B) PC90 (C) physical mixture (C)Lyophilized (DSF-IV8).

Fourier transform infrared spectroscopy (FTIR)

(Figure 7) shown the FTIR spectra of DSF, SPC90, the physical mixture, and DSF-IV8. The DSF spectra displayed distinct peaks at 2975 cm^{-1} (associated with the stretching vibration of C-H bonds), 1496 cm^{-1} (representing the N-C = S bond), 554 cm^{-1} (indicating the S-S bond), and 1273 cm^{-1} (referring to the C-S bond). The FTIR spectrum of DSF-IV8 shows the absence of the distinctive C-H bands, indicating a transformation from DSF bulk

medication to DSF-IV8. The presence of molecular interactions, specifically hydrogen bonds, between DSF and SPC90 is evident in the synthesis of DSF-IV8. Nevertheless, the fingerprint region of the DSF-IV8 exhibits all the distinctive peaks associated with DSF, indicating that its chemical structure remained identical during the production of the DSF-IV8 and retained its original chemical composition with SPC90^(53,54).



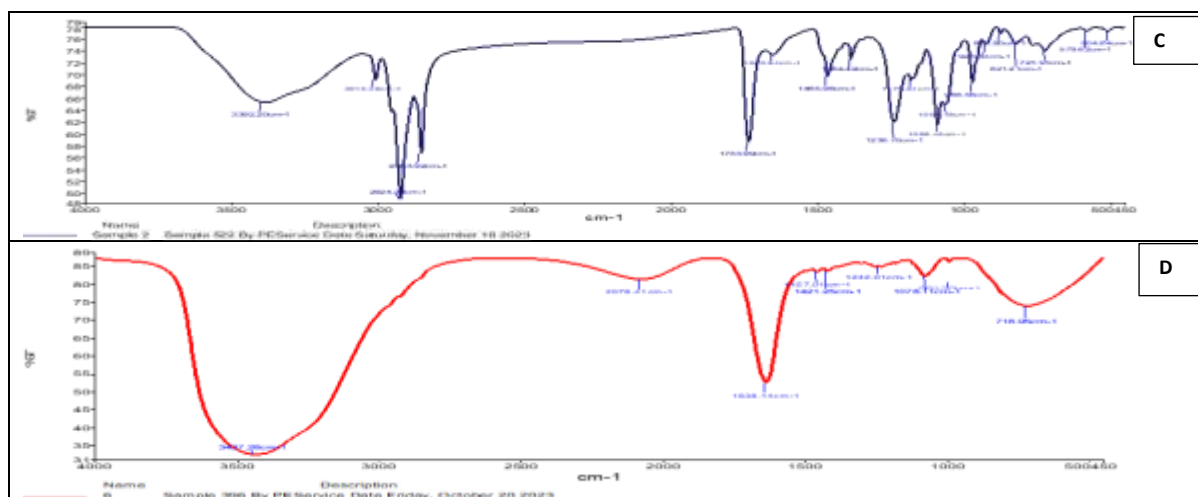


Figure 7. FTIR spectrum (A) Pure DSF (B)Phosphatidylcholine 90(C) Physical mixture (D) DSF-IV8.

Transmission electron microscopy of DSF-invasomes (TEM)

Microscopy images were obtained using a transmission electron microscope (TEM) as seen in Figure 8 at different magnification powers. The DSF-IV8 were observed in the TEM image as intact, spherical vesicles with a distinct shape and core, free

of any clumping, and exhibiting well-defined internal characteristics. The DSF-loaded invasomes appear to be within the nanometric size range, as confirmed by TEM observations, which matches the size measurements by dynamic light scattering⁽⁵⁵⁾.

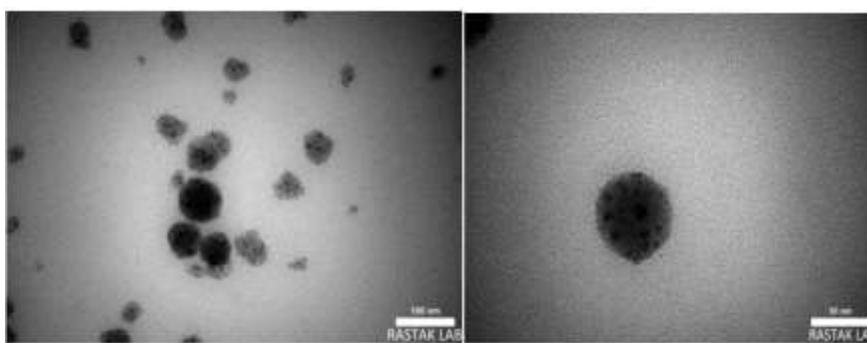


Figure 8. TEM image of optimized DSF-loaded invasomes formulation at different magnification power, DSF (Disulfiram)

Conclusion

Based on the data obtained from the present study, the study may draw the following conclusions: The disulfiram (DSF) can be effectively formulated as a nanoinvasome by thin film hydration method using carvacrol in 1% and SPC90 2%. DSF-IV8 exhibits superior entrapment efficacy and best release profile compared to pure disulfiram (DSF). The transmission electron microscopy (TEM) analysis showed that the particles had an almost perfect spherical shape with a distinct shape and core, free of any clumping, and exhibiting well-defined internal characteristics. The Fourier Transform Infrared (FTIR) analysis of the DSF-IV8 formula, established as a nanoinvasome, showed the compatibility between the drug and other excipients in the formula.

Acknowledgment

The authors thank the College of Pharmacy - University of Baghdad for their

support and for providing the necessary facilities to complete this research.

Conflicts of Interest

The authors stated no conflict of interest in the manuscript.

Funding

There is no financial support for this work.

Ethics Statements

There were no humans or animals used in all experiments.

Author Contribution

The author's responsibilities are described as follows: Preparation, collecting, and analyzing data: Worood Hameed. Designing, reviewing, and supervising the project: Hanan Jalal Kassab. All authors reviewed the results and approved the final version of the manuscript.

References

1. Jeong WY, Kwon M, Choi HE, Kim KS. Recent advances in transdermal drug delivery systems: A review. *Biomaterials research*. 2021 Dec; 25:1-5.
2. Ashoor JA, Mohsin JM, Mohsin HM, Mahde BW, Gareeb MM. Permeability Enhancement of Methotrexate Transdermal Gel using Eucalyptus oil, Peppermint Oil and Olive Oil (Conference Paper). *Iraqi Journal of Pharmaceutical Sciences*. 2021;30(Suppl.):16-21.
3. Ghasemiyeh P, Mohammadi-Samani S. Potential of nanoparticles as permeation enhancers and targeted delivery options for skin: Advantages and disadvantages. *Drug design, development, and therapy*. 2020 Aug 12;3271-89.
4. Kumar B, Pandey M, Aggarwal R, Sahoo PK. A comprehensive review on invasomal carriers incorporating natural terpenes for augmented transdermal delivery. *Future Journal of Pharmaceutical Sciences*. 2022 Dec 2;8(1):50.
5. Nangare S, Dugam S. Smart invasome synthesis, characterizations, pharmaceutical applications, and pharmacokinetic perspective: a review. *Future Journal of Pharmaceutical Sciences*. 2020 Dec;6(1):1-21.
6. Dumitriu Buzia O, Păduraru AM, Stefan CS, Dinu M, Cocos DI, Nwabudike LC, Tatu AL. Strategies for Improving Transdermal Administration: New Approaches to Controlled Drug Release. *Pharmaceutics*. 2023 Apr 7;15(4):1183.
7. Samir B, El-Kamel A, Zahran N, Heikal L. Resveratrol-loaded invasome gel: A promising nanoformulation for treatment of skin cancer. *Drug Delivery and Translational Research*. 2024 Feb 15:1-7.
8. Butcher K, Kannappan V, Kilari RS, Morris MR, McConville C, Armesilla AL, Wang W. Investigation of the key chemical structures involved in the anticancer activity of disulfiram in A549 non-small cell lung cancer cell line. *BMC cancer*. 2018 Dec;18(1):1-2.
9. Lu C, Li X, Ren Y, Zhang X. Disulfiram: a novel repurposed drug for cancer therapy. *Cancer Chemotherapy and Pharmacology*. 2021 Feb; 87:159-72.
10. Kannappan V, Ali M, Small B, Rajendran G, Elzhenni S, Taj H, Wang W, Dou QP. Recent advances in repurposing disulfiram and disulfiram derivatives as copper-dependent anticancer agents. *Frontiers in Molecular Biosciences*. 2021 Sep 17;8:741316.
11. Lajarin-Reinares M, Martinez-Estevé E, Pena-Rodríguez E, Cañellas-Santos M, Bulut S, Karabelas K, Clauss A, Nieto C, Mallandrich M, Fernandez-Campos F. The Efficacy and Biopharmaceutical Properties of a Fixed-Dose Combination of Disulfiram and Benzyl Benzoate. *International Journal of Molecular Sciences*. 2022 Sep 19;23(18):10969.
12. Tawari EP, Liu P, Wang Z, Kannappan V, Mcconville C, Armesilla A, Darling J, Irache J, Yoncheva K, Wang W, Petrov P. Pluronic micelle-encapsulated Disulfiram targets cancer stem-like cells and reverses pan-resistance in acquired resistant breast cancer cell lines. *Cancer Research*. 2015 Aug 1;75(15_Supplement):4067.
13. Mia F, Govender M, Indermun S, Kumar P, du Toit LC, Choonara YE. A nano-encapsulated-gel-composite for the treatment of alcohol abuse and addiction. *Nanofabrication*. 2022 Jun 20;7:e002.
14. Li H, Liu B, Ao H, Fu J, Wang Y, Feng Y, Guo Y, Wang X. Soybean lecithin stabilizes disulfiram nanosuspensions with a high drug-loading content: remarkably improved antitumor efficacy. *Journal of Nanobiotechnology*. 2020 Dec;18:1-1.
15. Ou AT, Zhang JX, Fang YF, Wang R, Tang XP, Zhao PF, Zhao YG, Zhang M, Huang YZ. Disulfiram-loaded lactoferrin nanoparticles for treating inflammatory diseases. *Acta Pharmacologica Sinica*. 2021 Nov;42(11):1913-20.
16. Najlah M, Said Suliman A, Tolaymat I, Kurusamy S, Kannappan V, Elhissi AM, Wang W. Development of injectable PEGylated liposome encapsulating disulfiram for colorectal cancer treatment. *Pharmaceutics*. 2019 Nov 14;11(11):610.
17. Yu S, Ni H, Xu X, Cai Y, Feng J, Zhang J. Subcutaneous Rapid Dissolution Microneedle Patch Integrated with CuO₂ and Disulfiram for Augmented Antimelanoma Efficacy through Multimodal Synergy of Photothermal Therapy, Chemodynamic Therapy, and Chemotherapy. *ACS Biomaterials Science & Engineering*. 2023 Oct 24;9(11):6425-37.
18. Motlagh MZ, Mahdavi N, Miri-Lavasani Z, Aminishakib P, Khoramipour M, Arki MK, Rezaei N, Hossein-Khannazer N, Vosough M. Disulfiram-loaded niosomes reduces cancerous phenotypes in oral squamous cell carcinoma cells. *Cell Journal (Yakhteh)*. 2023 Jun;25(6):407.
19. Anitha P, Satyanarayana SV. Design and optimization of nano invasomal gel of Glibenclamide and Atenolol combination: in vitro and in vivo evaluation. *Future Journal of Pharmaceutical Sciences*. 2021 Dec;7:1-8.
20. Tawfik MA, Eltaweel MM, Fatouh AM, Shamsel-Din HA, Ibrahim AB. Brain targeting of zolmitriptan via transdermal threesomes: statistical optimization and in vivo biodistribution study by ^{99m}Tc radiolabeling technique. *Drug Delivery and Translational Research*. 2023 Jun 5:1-8.

21. Suwanpidokkul N, Thongnopnua P, Umprayn K. Transdermal delivery of zidovudine (AZT): the effects of vehicles, enhancers, and polymer membranes on permeation across cadaver pig skin. *AAPS PharmSciTech*. 2004 Sep; 5:82-9.
22. Alzalzaalee R, Kassab H. Factors affecting the preparation of Cilnidipine nanoparticles. *Iraqi Journal of Pharmaceutical Sciences* (P-ISSN 1683-3597 E-ISSN 2521-3512). 2023 Nov 3;32(Suppl.):235-43.
23. Neamah MJ, Al-Akkam EJ. Preparation and characterization of vemurafenib microemulsion. *Iraqi Journal of Pharmaceutical Sciences* (P-ISSN 1683-3597 E-ISSN 2521-3512). 2023 Nov 4;32(Suppl.):316-25
24. Abonashay SG, Hassan HA, Shalaby MA, Fouad AG, Mobarez E, El-Banna HA. Formulation, pharmacokinetics, and antibacterial activity of florfenicol-loaded niosome. *Drug Delivery and Translational Research*. 2023 Nov 13:1-6.
25. Albash R, Al-Mahallawi AM, Hassan M, Alaa-Eldin AA. Development and optimization of terpene-enriched vesicles (Terpesomes) for effective ocular delivery of fenticonazole nitrate: in vitro characterization and in vivo assessment. *International Journal of Nanomedicine*. 2021 Jan 26:609-21.
26. Fasehee H, Dinarvand R, Ghavamzadeh A, Esfandyari-Manesh M, Moradian H, Faghihi S, Ghaffari SH. Delivery of disulfiram into breast cancer cells using folate-receptor-targeted PLGA-PEG nanoparticles: in vitro and in vivo investigations. *Journal of Nanobiotechnology*. 2016 Dec;14(1):1-8.
27. Jiapaer Z, Zhang L, Ma W, Liu H, Li C, Huang W, Shao S. Disulfiram-loaded hollow copper sulfide nanoparticles show anti-tumor effects in preclinical models of colorectal cancer. *Biochemical and Biophysical Research Communications*. 2022 Dec 20;635:291-8.
28. Albassam NY, Kassab HJ. Diacerein loaded nova some for transdermal delivery: Preparation, in-vitro characterization and factors affecting formulation. *Iraqi Journal of Pharmaceutical Sciences* (P-ISSN 1683-3597 E-ISSN 2521-3512). 2023 Nov 3;32(Suppl.):214-24
29. Tawfik MA, Tadros MI, Mohamed MI, Nageeb El-Helaly S. Low-frequency versus high-frequency ultrasound-mediated transdermal delivery of agomelatine-loaded invasomes: development, optimization and in-vivo pharmacokinetic assessment. *International journal of nanomedicine*. 2020 Nov 12:8893-910
30. Al-Edhari GH, Al Gawhari FJ. Study the Effect of Formulation Variables on the Preparation of Nisoldipine Loaded Nano Bilosomes. *Iraqi Journal of Pharmaceutical Sciences* (P-ISSN 1683-3597 E-ISSN 2521-3512). 2023 Nov 4;32(Suppl.):271-82.
31. Tamer Ma, Kassab HJ. The Development of A Brain-Targeted Mucoadhesive Amisulpride-Loaded Nanostructured Lipid Carrier. *Farmacia*. 2023 Sep 1;71(5).
32. Ali SK, Al-Akkam EJ. Bilosomes as Soft Nanovesicular Carriers for Ropinirole Hydrochloride: Preparation and In-vitro Characterization. *Iraqi Journal of Pharmaceutical Sciences* (P-ISSN 1683-3597 E-ISSN 2521-3512). 2023 Nov 3;32(Suppl.):177-87.
33. Ala'a DN, Rajab NA. Formulation and characterization of niosomes for controlled delivery of tolmetin. *Journal of Pharmaceutical Negative Results*. 2022 Oct 7;13(4):159-69.
34. Danaei M, Dehghankhold M, Ataei S, Hasanazadeh Davarani F, Javanmard R, Dokhani A, Khorasani S, Mozafari MR. Impact of particle size and polydispersity index on the clinical applications of lipidic nanocarrier systems. *Pharmaceutics*. 2018 May 18;10(2):57.
35. Guillot AJ, Martínez-Navarrete M, Garrigues TM, Melero A. Skin drug delivery using lipid vesicles: A starting guideline for their development. *Journal of Controlled Release*. 2023 Mar 1;355:624-54.
36. Hoda Q, Aqil M, Ahad A, Imam SS, Praveen A, Qadir A, Iqbal Z. Optimization of valencene containing lipid vesicles for boosting the delivery of itraconazole. *3 Biotech*. 2021 Mar;11:1-3.
37. Sapra B, Jain S, Tiwary AK. Percutaneous permeation enhancement by terpenes: mechanistic view. *The AAPS journal*. 2008 Mar;10:120-32.
38. Wang L, Dekker M, Heising J, Fogliano V, Berton-Carabin CC. Carvacrol release from PLA to a model food emulsion: Impact of oil droplet size. *Food Control*. 2020 Aug 1;114:107247.
39. Ben Arfa A, Combes S, Preziosi-Belloy L, Gontard N, Chalier P. Antimicrobial activity of carvacrol related to its chemical structure. *Letters in applied microbiology*. 2006 Aug 1;43(2):149-54.
40. Amnuaikit T, Limsuwan T, Khongkow P, Boonme P. Vesicular carriers containing phenylethyl resorcinol for topical delivery system; liposomes, transfersomes and invasomes. *Asian Journal of Pharmaceutical Sciences*. 2018 Sep 1;13(5):472-84.
41. Andrade J, González-Martínez C, Chiralt A. Liposomal encapsulation of carvacrol to obtain active poly (vinyl alcohol) films. *Molecules*. 2021 Mar 13;26(6):1589.
42. Dragicevic-Curic N, Gräfe S, Albrecht V, Fahr A. Topical application of temoporfin-loaded invasomes for photodynamic therapy of subcutaneously implanted tumours in mice: a pilot study. *Journal of photochemistry and*

- photobiology B: Biology. 2008 Apr 25;91(1):41-50.
43. El-Shenawy AA, Abdelhafez WA, Ismail A, Kassem AA. Formulation and characterization of nanosized ethosomal formulations of antigout model drug (febuxostat) prepared by cold method: In vitro/ex vivo and in vivo assessment. Aaps Pharmscitech. 2020 Jan; 21:1-3.
 44. He H, Yuan D, Wu Y, Cao Y. Pharmacokinetics and pharmacodynamics modeling and simulation systems to support the development and regulation of liposomal drugs. Pharmaceutics. 2019 Mar 7;11(3):110.
 45. El-Tokhy FS, Abdel-Mottaleb MM, El-Ghany EA, Geneidi AS. Design of long-acting invasomal nanovesicles for improved transdermal permeation and bioavailability of asenapine maleate for the chronic treatment of schizophrenia. International Journal of Pharmaceutics. 2021 Oct 25; 608:121080.
 46. Laothaweerungsawat N, Neimkhum W, Anuchapreeda S, Sirithunyalug J, Chaiana W. Transdermal delivery enhancement of carvacrol from *Origanum vulgare* L. essential oil by microemulsion. International Journal of Pharmaceutics. 2020 Apr 15;579:119052.
 47. Heckler C, Silva CM, Cacciatore FA, Daroit DJ, da Silva Malheiros P. Thymol and carvacrol in nanoliposomes: Characterization and a comparison with free counterparts against planktonic and glass-adhered *Salmonella*. Lwt. 2020 Jun 1;127:109382.
 48. Sayed OM, Abo El-Ela FI, Kharshoum RM, Salem HF. Treatment of basal cell carcinoma via binary ethosomes of vismodegib: in vitro and in vivo studies. AAPS PharmSciTech. 2020 Feb;21:1-1.
 49. Fox LT, Gerber M, Plessis JD, Hamman JH. Transdermal drug delivery enhancement by compounds of natural origin. Molecules. 2011 Dec 16;16(12):10507-40.
 50. El-Nabarawi MA, Shamma RN, Farouk F, Nasralla SM. Dapsone-loaded invasomes as a potential treatment of acne: preparation, characterization, and in vivo skin deposition assay. Aaps Pharmscitech. 2018 Jul;19:2174-84.
 51. Pereira AM, Kaya A, Alves D, Ansari-Fard N, Tolaymat I, Arafat B, Najlah M. Preparation and characterization of disulfiram and beta cyclodextrin inclusion complexes for potential application in the treatment of SARS-CoV-2 via nebulization. Molecules. 2022 Aug 31;27(17):5600.
 52. Tyukova VS, Kedik SA, Panov AV, Zhavoronok ES, Mendelev DI, Senchikhin IN, Fursova AZ, Rumyantseva YV, Kolosova NG. Synthesis of a Disulfiram Inclusion Complex with Hydroxypropyl- β -Cyclodextrin and Its Effect on Cataract Development in Rats. Pharmaceutical Chemistry Journal. 2020 Mar;53:1158-63.
 53. Trivedi MK, Branton A, Trivedi D, Nayak G, Bairwa K, Jana S. Spectroscopic characterization of disulfiram and nicotinic acid after biofield treatment. J Anal Bioanal Tech. 2015 Aug 14;6(265):2.
 54. Zhang C, Xu T, Zhang D, He W, Wang S, Jiang T. Disulfiram thermosensitive in-situ gel based on solid dispersion for cataract. Asian journal of pharmaceutical sciences. 2018 Nov 1;13(6):527-35.
 55. Fouad AG, Ali MR, Naguib DM, Farouk HO, Zanaty MI, El-Ela FI. Design, optimization, and in vivo evaluation of invasome-mediated candesartan for the control of diabetes-associated atherosclerosis. Drug Delivery and Translational Research. 2023 Aug 21:1-7.

تأثير أنواع مختلفة من التيربينات على تحضير الدايسلفيرام المحمل في حويصلات الانفاسوم للتوصيل عبر الجلد تحضير وتقييم خارج الجسم ورود حميد الزهيري¹ و خان جلال كساب^{2*}

¹ فرع الصيدلانيات، كلية الصيدلة، جامعة الاسراء، بغداد، العراق.

² فرع الصيدلانيات، كلية الصيدلة، جامعة بغداد، بغداد، العراق.

الخلاصة

الإنفاسومات هي أنظمة حويصلية جديدة تظهر قدرة محسنة على اختراق الجلد مقارنة بالليبوسومات التقليدية. تحتوي هذه الحويصلات على فسفوليبيدات وإيثانول وتبرين في هياكلها؛ حيث تمنح هذه المكونات خصائص مناسبة لاختراق الجلد للحويصلات الرقيقة. الدايسلفيرام (DSF) هو مشتق ثيوكاربامات تم استخدامه لعلاج الإدمان على الكحول ويمكن استخدامه أيضاً لعلاج الأورام. الهدف من هذه الدراسة هو تطوير إنفاسوم ديسلفيرام كحامل حويصلي وتقييم تأثير متغيرات التركيب المختلفة، مثل نوع وكمية التيربينات (الليمونين والسيرترال والكافراول)، على حجم الجسيمات وكفاءة الاحتجاز ومؤشر التشتت للإنفاسومات المحضرة. تم اختيار تشتت الإنفاسوم المحسن الذي يحتوي على كفاءة احتجاز أكثر من 70٪ لدراسة الإطلاق في المختبر. تم تحضير إنفاسومات ديسلفيرام بنجاح باستخدام تقنية الترطيب بالغشاء الرقيق. تم تطوير تسع صيغ لإنفاسومات لإعداد تشتت إنفاسوم ديسلفيرام. أظهر تشتت الإنفاسوم المختار (DSF-IV8) الذي يظهر نسبة أعلى من إطلاق DSF فعالية أكبر، وقد تم تحليله بالإضافة إلى ذلك لخصائصه الأمثل، بما في ذلك حويصلات كروية بحجم جسيم 2.2 ± 119.2 نانومتر، ومؤشر تشتت 0.05 ± 0.18 ، وكفاءة احتجاز $95.3 \pm 0.8\%$ ، و 96.32% من إطلاق DSF من تشتت الإنفاسوم بعد 24 ساعة، وقد تم قياس قيمة الجهد الكهربائي زيتا لتكون -33.6 ± 1.6 مللي فولت، وأظهر تحليل FTIR التوافق بين الدواء والمكونات الأخرى في التركيبة. أظهرت صور TEM حويصلات DSF-IV8 شكل ثابت، وشكل كروي، خالية من أية تجمعات، وتظهر خصائص داخلية جيدة التعريف. في النهاية، أظهرت تقنية الترطيب بالغشاء الرقيق فعالية في صياغة تشتت إنفاسوم.

الكلمات المفتاحية :- طريقة الاعطاء عن طريق الجلد، إنفاسوم، الدايسلفيرام، التبرين، الكافراول.